Inhibitor selectivity: profiling and prediction

Janssen, A.P.A.

If the elements are the alphabet of chemistry, then the compounds are its plays, its poems, and its novels.
Peter Atkins

2 Hit-to-lead optimization of triazole sulfonamide DAGL-α inhibitors

Introduction

Diacylglycerol lipase (DAGL)-α and DAGL-β inhibitors have been under active investigation as potential drugs for the treatment of metabolic and neurodegenerative disorders for nearly a decade.[1,2] The recent generations of optimized inhibitors can be divided in three chemotypes: the α-ketoheterocycles (LEI104 and LEI105[3,4]), the glycine sulfonamides (*e.g.* LEI106)[5,6] and the triazole ureas (KT109, D034 and DH376[7,8]). These inhibitors have been used successfully in a variety of cellular and animal models to study the effect of DAGL inhibition in detail.[1,4,7–9] However, as potential drugs, each of these

inhibitor classes has its own set of shortcomings. The α-ketoheterocycles are the most selective inhibitors published to date, with no known off-targets reported for LEI105.[4] However, LEI105 has a very low oral bioavailability due to its low solubility and high metabolic clearance (unpublished data). The glycine sulfonamides are dual DAGL and α/β-hydrolase domain containing protein 6 (ABHD6) inhibitors, and have a few further unidentified off-targets *in vitro*.[5] The free acid of the glycine moiety was found to be crucial for activity, but likely caused the observed significantly reduced cellular potency and low brain penetration.[9] Although the triazole urea derivatives DO34 and DH376 are less lipophilic and more selective than the original hit KT109[1], they still have several other serine hydrolases as off-targets. In all, the current state-of-the-art for DAGL inhibitors leaves room for improvement and warrants the search for new chemical scaffolds.

To find new hits for DAGL-α, a high throughput screening campaign was performed in collaboration with the Pivot Park Screening Centre and the European Lead Factory.[10] Initial screening at 10 μM in a previously reported surrogate substrate assay yielded 1932 hits (Figure 2.1).[3] These were confirmed at a lower concentration (1.25 μM) and verified in an orthogonal activity-based protein profiling (ABPP) assay. After final selections based on purity and legal restrictions, 46 qualified hits were disclosed. This set of compounds yielded a series of 1,2,4-triazole-3-sulfon(amide) urea inhibitors (**1**-**3**, Figure 2.1) that was selected for further optimization, because of its promising physicochemical properties (**1**: CLogP = 2.07, tPSA = 85.6, MW = 337). Here, the results of the structure activity relationship (SAR) investigations are described, leading to the most polar *in vivo* active triazole urea DAGL inhibitor reported to date.

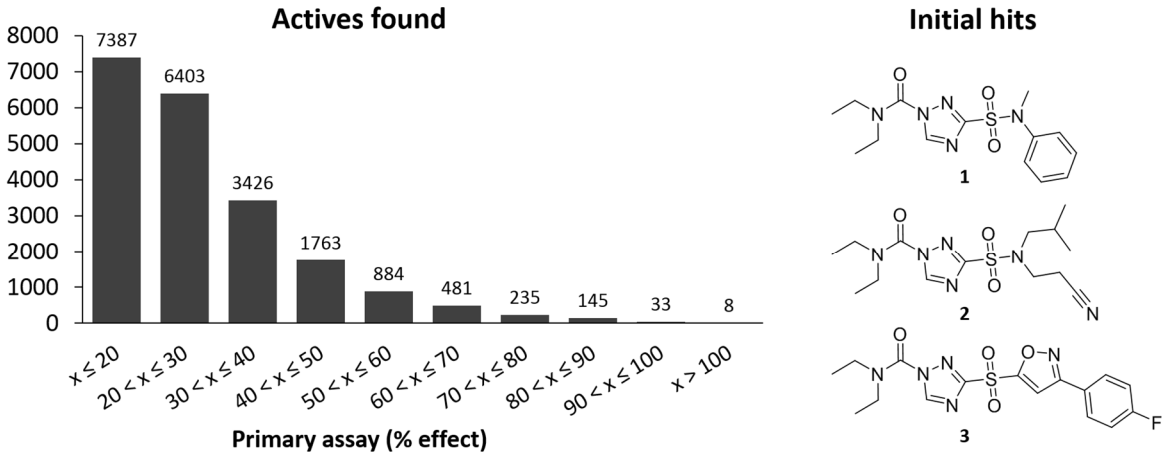

Compounds			% Total
Total screened	302.655	-	100
Primary assay hits	1.932	> 50% eff. (10 μM)	0.64
Active confirmation hits	263	> 70% eff. (10 μM) > 50% eff. (1.25 μM)	0.09
Triaging and orthogonal assay	46	Chemical eye, clustering, legal, purity	0.02

Figure 2.1 | Summary of the high throughput screening campaign for DAGL-α. The triazole sulfonamide series was selected from the initial hits to be further optimized.

Results and discussion

To investigate the SAR of the triazole-sulfonamide-ureas a library of 65 compounds was synthesized at the European Lead Factory and screened using a previously reported colorimetric DAGL-α surrogate substrate assay.[3] The SAR is described in a topological fashion below. The initial variations focussed on finding the minimal requirements of the scaffold to inhibit DAGL-α (Table 2.1). The desired polar core of the scaffold was maintained, while varying the substituents on the sulfonamide (**1**-**8**) and on the urea moiety (**9**-**25**). Removal of one (**4**) or both (**5**) sulfonamide substituents significantly reduced DAGL-α inhibitory activity. Piperidine- (**6**) and morpholine- (**7**) substituted sulfonamides lost potency, while an inhibitor substituted with two isobutyl groups (**8**) was tolerated. This suggested that conformational flexibility and/or a lipophilic substituent on the sulfonamide is beneficial for the inhibitory activity.

Changing the diethyl substitution at the urea to a monomethyl (**9**), monoethyl (**10**) or di-methoxyethyl (**11**) group abolished activity against DAGL-α, but the dimethylamine (**12**) was active. Cyclization of the diethylamine substituents to pyrrolidine (**13**) or piperidine (**14**), but not morpholine (**15**) or 4-methylpiperazine (**16**), was tolerated. Even when decorated with a benzyl, mono-substituted amines failed to inhibit DAGL-α (**17** and **18**). Decorating the cyclic amines with a 3-phenyl or 2-benzyl substituent (**19**-**21**), but not a 2-phenyl (**22** and **23**), greatly improved binding to DAGL-α yielding a single digit nanomolar potent inhibitor (**21**). This is in line with the observations made by Hsu *et al*. in the optimization towards KT109[11] and suggests that 2-benzyl piperidine is a preferred motif for DAGL and the binding mode of this 3-substituted 1,2,4-triazole urea scaffold is comparable to that of the 4-substituted 1,2,3-triazole ureas. The loss of activity for compounds **24** and **25** further illustrates the lipophilic nature of the binding pocket.

Next the sulfonamide substitution pattern was further explored using the 3-phenyl-pyrrolidine, the 2-benzylpyrrolidine and the 2-benzylpiperidine as substituents on the amine urea for matched-molecular pair analysis (Table 2.2, **26**-**51**). In general, it was found that the 2-benzylpyrrolidine series (**19**, **26**-**33**) was the least active, while the 2-benzylpiperidine series (**21**, **45**-**51**) delivered the most active inhibitors. The SAR trend within each series was generally consistent across the three chemotypes. It was found that the increase in the size of the cycloalkyl substituent on the sulfonamide provided more active compounds. Virtually all methyl substituted variants (**19**-**21**, **26**-**28, 34**-**37** and **45**-**46**) were more potent than their hydrogen counterparts (**29**-**33**, **38**-**44** and **47**-**51,** respectively). None of the sulfonamide variants, however, provided an improvement over the originally found methyl aniline in **19**-**21**.

Finally, to investigate the necessity of the sulfonamide moiety a small selection of sulfide, sulfoxide and sulfone variants (**52**-**65**, Table 2.3) was tested. The sulfonamide was not required for potent inhibitory activity (e.g. **58**, **60**, **64** and **65**) and oxidation of the sulfur significantly increased the potency of the inhibitors (e.g. **52, 53** and **54** or **55** vs. **56**, **57** vs. **58**, **59** vs. **60** and **61** vs. **62**).

Table 2.1 | Initial variations of the sulfonamide substitution and urea bound amine groups. pIC_{50}s were determined by a surrogate substrate assay using membrane fractions of hDAGL-α overexpressing HEK293T cells, and are reported as mean of N=2, n=2 experiments.

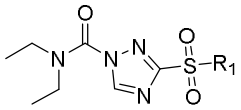

#	R_1	pIC_{50} DAGL-α
1	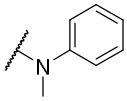	5.9
2	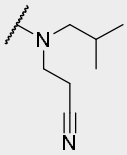	5.5
4	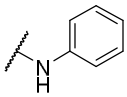	5.5
5		< 5
6	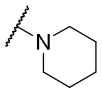	5.2
7	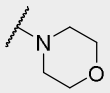	< 5
8	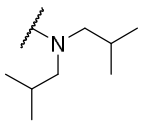	5.9

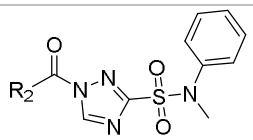

#	R_2	pIC_{50} DAGL-α	#	R_2	pIC_{50} DAGL-α
1	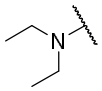	5.9	17	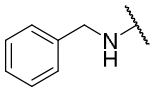	< 5
9		< 5	18	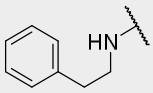	< 5
10	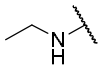	< 5	19	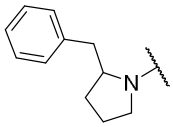	7.5
11	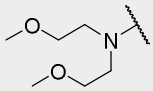	5.8	20	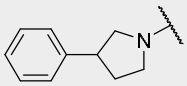	7.5
12		6.2	21	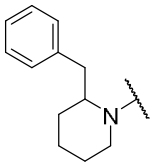	8.6
13		6.2	22	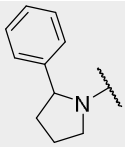	5.4
14	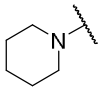	6.1	23	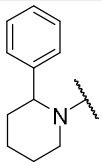	6.2
15	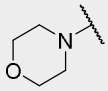	5.0	24	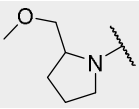	5.8
16	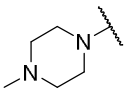	< 5	25	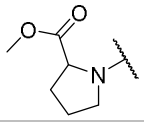	< 5

Table 2.2 | Sulfonamide variations for the three most promising retaining groups. pIC_{50}s were determined by a surrogate substrate assay using membrane fractions of hDAGL-α overexpressing HEK293T cells, and are reported as mean of N=2, n=2 experiments.

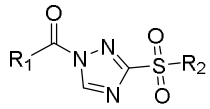

R_1	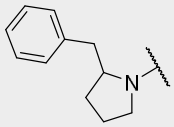		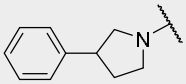		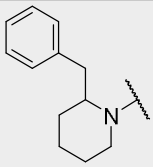	
R_2	#	pIC_{50} DAGL-α	#	pIC_{50} DAGL-α	#	pIC_{50} DAGL-α
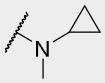	**26**	6.0	**34**	6.9		-
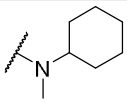	**27**	5.9	**35**	7.9	**45**	7.6
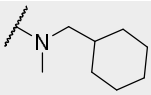	**28**	7.0	**36**	8.0	**46**	8.1
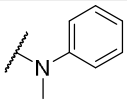	**19**	7.5	**20**	7.5	**21**	8.6
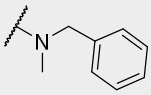		-	**37**	7.2		-
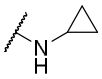		-	**38**	6.5		-
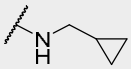	**29**	6.0	**39**	7.1	**47**	7.2
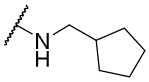	**30**	6.7	**40**	7.4	**48**	7.8
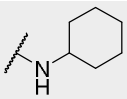	**31**	6.9	**41**	7.6	**49**	7.6
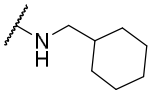	**32**	6.8	**42**	7.6	**50**	7.5
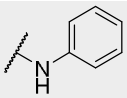	**33**	6.9	**43**	6.9	**51**	7.5
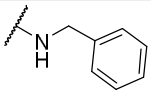		-	**44**	7.2		-

Table 2.3 | Sulfide, sulfone and sulfoxide variations for the two most promising urea substitutions. pIC_{50}s were determined by a surrogate substrate assay using membrane fractions of hDAGL-α overexpressing HEK293T cells, and are reported as mean of N=2, n=2 experiments.

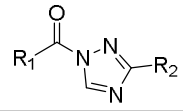

R_1	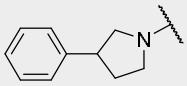		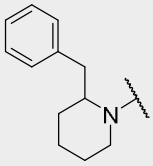	
R_2	#	pIC_{50} DAGL-α	#	pIC_{50} DAGL-α
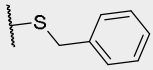	**52**	6.1	**61**	6.6
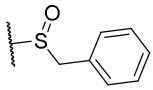	**53**	6.5		-
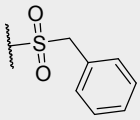	**54**	7.7	**62**	7.8
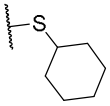	**55**	5.8		-
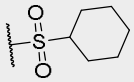	**56**	7.3	**63**	7.3
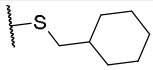	**57**	6.0		-
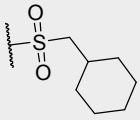	**58**	8.0	**64**	8.0
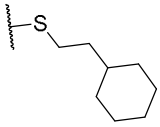	**59**	5.8		-
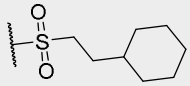	**60**	8.0	**65**	8.0

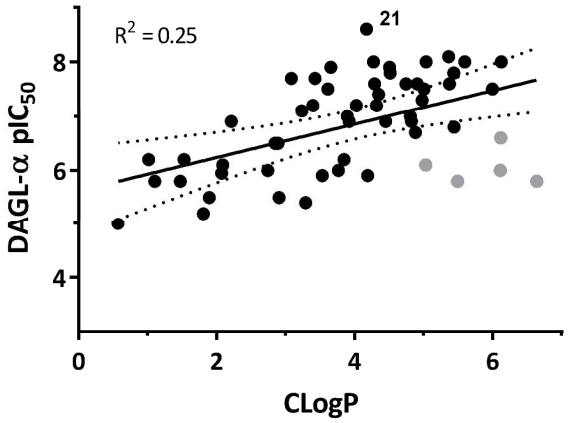

Figure 2.2 | Correlation analysis of calculated lipophilicity (CLogP) and measured pIC_{50} for DAGL-α. Grey markers denote sulfide compounds **52**, **55**, **57**, **59** and **61**. Regression line with 99% confidence interval is shown.

For all compounds the CLogP was calculated (Chemdraw 16.0) and plotted against the potency (pIC_{50}) for a correlation analysis (Figure 2.2). Although in general lipophilic groups tended to increase potency, only a poor correlation with an R^2 of 0.25 was found. This indicates that the potency of the inhibitors might not only be dependent on an increase in entropy due to the de-solvation effect, but may also reflect enthalpic interactions and steric clashes with the enzyme. The most notable example is the sulfide series (**52**, **55**, **57**, **59**, **61**; grey markers in Figure 2.2), which indicated that the sulfone-oxygen atoms present in the sulfonamide and sulfone variants and not present in the sulfides have a positive contribution to the overall potency, potentially due to an increased electron withdrawing character. Compound **21** truly stands out in this plot, showcasing its large lipophilic efficiency (LipE = 4.4), which is only surpassed by a few more promiscuous molecules like **12** (Figure 2.3).

Off-target profiling

Next all compounds were screened for off-targets using activity-based protein profiling (ABPP). Two broad spectrum activity-based probes (ABPs) were used: the commercially available FP-TAMRA (ActiveX®) and the tailored ABP MB064, which together label most of the endocannabinoid serine hydrolases. This approach uniquely enables the medicinal chemistry program to focus not only on potency in the primary assay, but also to be steered towards the more selective compounds. Initial screening was performed at 10 μM inhibitor concentration, but for the more active compounds (pIC_{50} > 7.5) the screening was repeated at 100 nM. A typical screening result is displayed in Figure S2.1. A direct comparison of the most promising compounds is shown in Figure 2.3. The ABPP-data indicate that the 3-phenylpyrrolidine series is more promiscuous than the 2-benzylpyrrolidines and especially the 2-benzylpiperidines. The latter series shows a dramatic reduction in inhibitory activity against several enzymes, among which ABHD16A, ABHD12 and FAAH. In all, compound **21** was selected for further biological profiling, as it displayed the highest overall activity (pIC_{50} = 8.6), large lipophilic efficiency (LipE = 4.4) and relatively good *in vitro* selectivity.

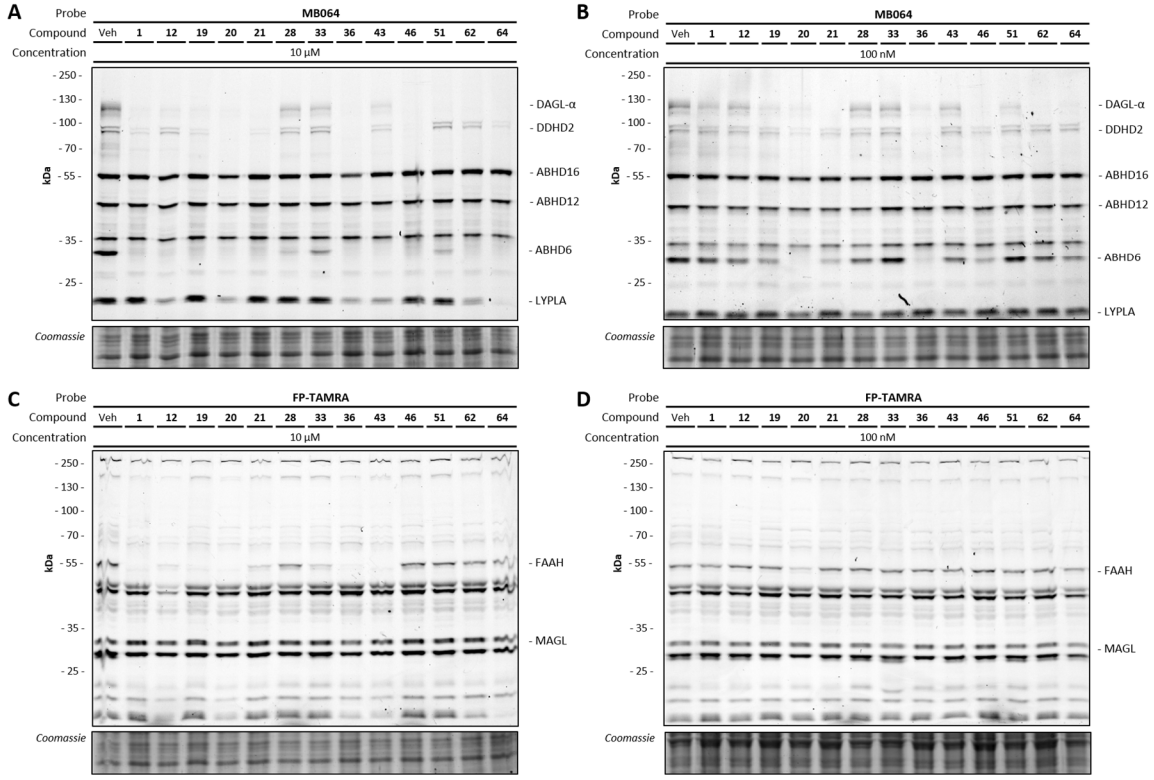

Figure 2.3 | Inhibition profiling of a selection of potent inhibitors in Table 2.1, 2.2 and 2.3 in *in vitro* treated mouse brain membrane proteome. Profiling was performed at compound concentrations of 10 µM (A, C) and 100 nM (B, D), using MB064 (A, B) and FP-TAMRA (C, D) for protein labeling.

Resynthesis of **21** and its activity-based probe (**77**)

Resynthesis of **21** was performed to enable further biological studies and was performed analogous to the synthetic methods used for the library synthesis (Scheme 2.1). In brief, 2-benzylpyridine (**66**) was hydrogenated using platinum oxide to yield the 2-benzyl-piperidine (**67**). In parallel, 1,2,4-triazole-3-thiol (**68**) was benzylated using benzylbromide. These were coupled in a triphosgene mediated coupling reaction to yield the triazole urea **70**. In a one-pot reaction the thioether was oxidized by *in situ* generated Cl_2 (from HCl and NaOCl) to the sulfonyl chloride, which was trapped by the addition of a large excess of *N*-methylaniline. This furnished **21** in moderate overall yield.

To use the covalent mode of action of these inhibitors to visualize target engagement, a two-step activity-based probe was designed (**77**, Scheme 2.1). This was done by fusing the previously described 5-propargylether substituted (S)-2-benzylpiperidine (**76**) of DH376 to the 1,2,4-triazole sulfonamide leaving group (**74**).[8] To this end, a new synthetic procedure was developed wherein the triphosgene coupling featured as the last step, to avoid putting the valuable chiral 2-benzyl piperidine through the harsh and low yielding chlorination step. The benzylated 1,2,4-triazole-3-thiol (**69**) was coupled to commercially available diphenylcarbamic chloride (**71**), before being reacted with chlorine and *N*-methylaniline. The urea moiety was then hydrolyzed using strong base and the resulting 1,2,4-triazole sulfonamide was coupled to the deprotected 5-substituted 2-benzylpiperidine (**76**), yielding **77**.

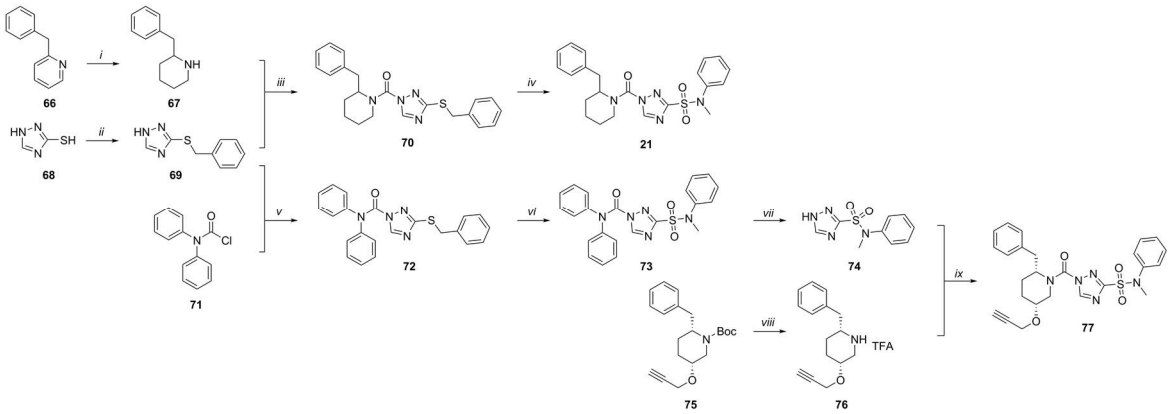

Scheme 2.1 | Synthesis of **21** and **77**. Synthesis of **75** was described in Deng *et al*.[8] Reagents and conditions: *i*) H_2, HCl, PtO_2, EtOH, 2 bar, 18 h, 64%; *ii*) benzylbromide, DMF, 18 h, 98%; *iii*) **67**, triphosgene, TEA, DCM, -5 °C → RT, 2 h, then **69**, K_2CO_3, DMF, 18 h, 32%; *iv*) HCl, NaOCl, DCM, -10 °C, 30 min, then *N*-methylaniline, -10 °C → RT, 2h, 52%; *v*) **69**, **71**, DIPEA, DMAP, THF, 65 °C, 5 h, 88%; *vi*) HCl, NaOCl, DCM, -10 °C, 20 min, then *N*-methylaniline, -10 °C → RT, 2h, 69%; *vii*) KOH, H_2O/THF (1:1), 18 h, 53%; *viii*) TFA, DCM, 5 h; *ix*) **76**, triphosgene, DIPEA, DCM, 0 °C → RT, 1 h, then **74**, DMAP, DIPEA, THF, 65 °C, 5 h, 67%.

Full *in vitro* and *in situ* profiling of **21** and **77**

Next, two orthogonal assays were performed to verify the activity of **21** and **77**. First, **21** and **77** were profiled in a competitive ABPP setting in a dose response fashion. Second, the compounds were tested in a previously developed natural substrate assay.[12] The resulting inhibition data are displayed in Table 2.4. Both compounds showed a slight reduction of potency in the competitive ABPP assay, compared to the surrogate substrate (PNP) assay, which could be due to a species difference as the surrogate substrate assay utilized human DAGL-α, whereas the ABPP assay was performed on mouse brain proteome. Both compounds showed a moderate selectivity *in vitro* over the major off-target ABHD6 of approximately 100-fold. In the natural substrate assay the activity of (human) DAGL-α was less potently inhibited, in line with previously reported observations.

The cellular activity of both compounds was tested in mouse Neuro-2a cells. Cells were treated with the compounds for one hour before the cells were harvested and analyzed by gel-based ABPP. The resulting gels (Figure 2.4) and quantification (Table 2.4) showed a similar potency for mouse DAGL-β *in situ* as for DAGL-α in the natural substrate assay, with a pIC_{50} of 6.5 and 7.2 for **21** and **77**, respectively. The potency for ABHD6 is remarkably increased to the single-digit nanomolar range, which is evidence of efficient cellular penetration of the compounds.

Table 2.4 | Activity data for **21** and **77** in the used biochemical and ABPP assays. Values are reported as mean ± standard deviation of N=3 (for ABPP) or N=2, n=2 (for PNP- and SAG-assay) replicates.

Compound	pIC_{50} DAGL-α PNP-assay	pIC_{50} DAGL-α ABPP-assay	pIC_{50} ABHD6 ABPP-assay	pIC_{50} DAGL-α SAG-assay	pIC_{50} DAGL-β *in situ*-assay
21	8.6 ± 0.3	8.1 ± 0.1	6.1 ± 0.1	6.4 ± 0.2	6.5 ± 0.1
77	8.6 ± 0.2	8.5 ± 0.1	6.8 ± 0.1	7.4 ± 0.1	7.2 ± 0.1

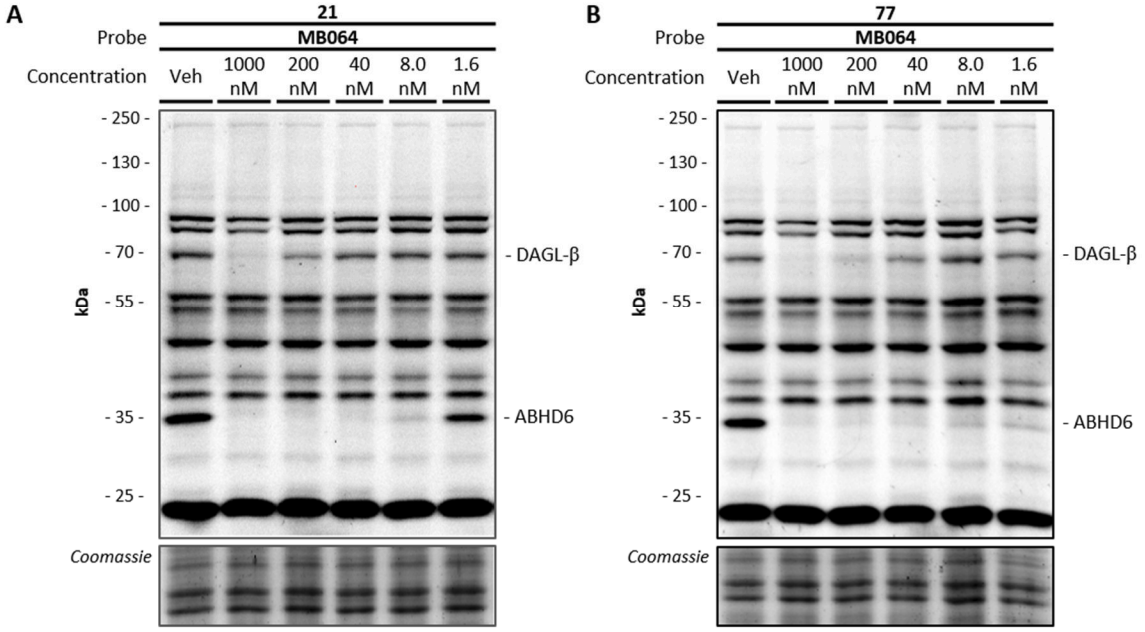

Figure 2.4 | Neuro-2a cells treated *in situ* with **21** (A) and **77** (B), labeled post-lysis with MB064 (2 μM, 20 min, RT). Coomassie was used for protein loading control.

21 and **77** are *in vivo* active

Considering the favourable physicochemical properties, *in vitro* and *in situ* potency and relatively high selectivity, both compounds were tested in mice to assess their *in vivo* target engagement. To this end, the compounds were administered intraperitoneal, using a high dose of 50 mg/kg of compound or vehicle (18:1:1 (v/v/v) saline:ethanol:PEG-40). The mice were sacrificed after two hours and the organs were harvested. Both the brain and the spleen were selected to assess target engagement of DAGL-α/β and ABHD6 in the central nervous system and peripheral organs. To visualize residual protein activity, the membrane proteomes were treated with both MB064 and FP-TAMRA (Figure 2.5). Compounds **21** and **77** abolished or reduced the fluorescent labeling of DAGL-α and ABHD6. This indicated that the compounds are *in vivo* active and are able to cross the blood-brain barrier. **77** was less active than **21**, as judged by the only partial inhibition of DAGL-α (Figure 2.5A). Both compounds seem to be quite selective, but **21** at this high dose also inhibited FAAH (band at 60 kDa labeled by FP-TAMRA). In the spleen the number of off-targets observed was somewhat higher. The strong band disappearing at 60 kDa is likely a group of carboxylic esterases, which are well-known to bind these types of inhibitors.[7,13] The labeling of DAGL-β in the spleen was faint, but inhibited by **21**.

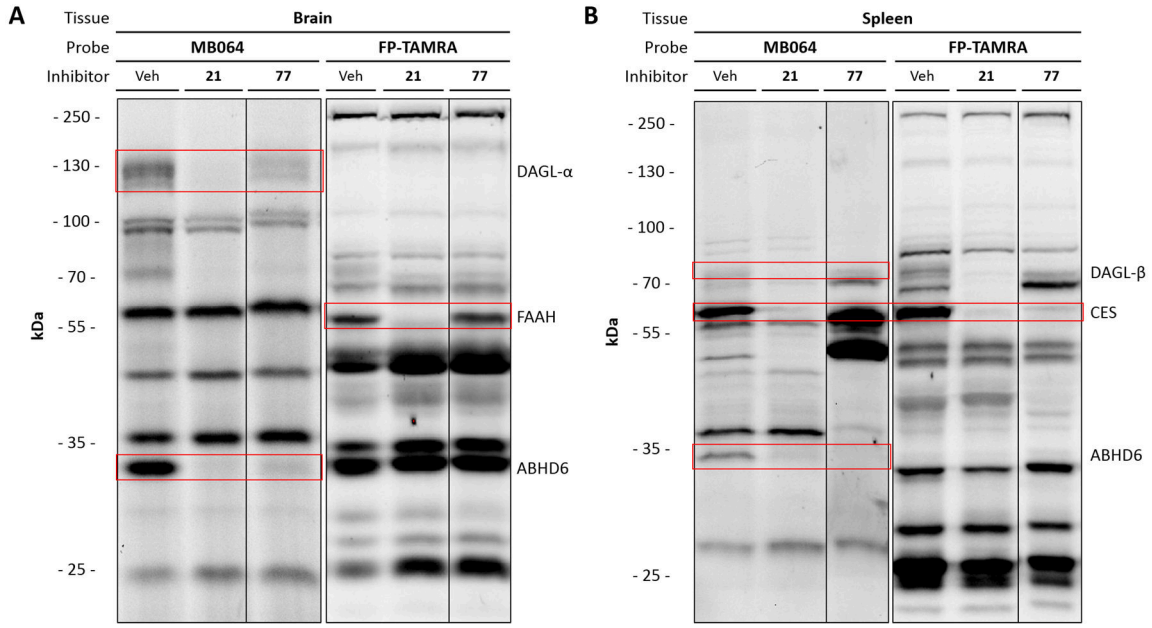

Figure 2.5 | Membrane fractions of mouse brain (A) and spleen (B) treated *in vivo* i.p. with 50 mg/kg of **21** and **77**, post-lysis labeled with MB064 or FP-TAMRA. Red boxes denote assigned bands (labels on the right of the gels).

Conclusion

All together, the discovery and optimization of a new series of DAGL inhibitors, based on a 1,2,4-triazole urea sulfonamide scaffold was reported in this Chapter. The optimized inhibitors had favourable physicochemical properties leading to a high lipophilic efficiency. Activity-based protein profiling was used to guide the optimization of potency and selectivity in parallel on endogenously expressed enzymes in brain lysates. Compound **21** proved cellular active and demonstrated *in vivo* activity in mice. Further dose-response studies have to be performed to establish the minimum dose required for complete DAGL-α inhibition in the brain.

Acknowledgements

The research received support from the Innovative Medicines Initiative Joint Undertaking grant n' 115489, resources are composed of financial contribution from the European Union's Seventh Framework Programme (FP7 / 2007-2013) and EFPIA companies' in-kind contribution. Freek Janssen, Marc Baggelaar, Hui Deng and Bobby Florea are kindly acknowledged for their help in the experimental parts of this research.

Methods

Chemical Biology Methods

Cell Culture

HEK293T (human embryonic kidney) and Neuro-2a (mouse neuroblastoma) cells were cultured at 37 °C under 7% CO_2 in DMEM containing phenol red, stable glutamine, 10% (v/v) New Born Calf Serum (Thermo Fisher), and penicillin and streptomycin (200 µg/mL each; Duchefa). Medium was refreshed every 2-3 days and cells were passaged twice a week at 80-90% confluence by resuspension in fresh medium.
Cells lines were purchased from ATCC and were regularly tested for mycoplasma contamination. Cultures were discarded after 2-3 months of use.

Transient transfection

One day prior to transfection HEK293T cells were seeded to 15-cm dishes (~62.500 cells/cm^2). Prior to transfection, culture medium was aspirated and a minimal amount of medium was added. A 3:1 (m/m) mixture of polyethyleneimine (PEI) (60 µg/dish) and human DAGL-α plasmid DNA (20 µg/dish) was prepared in serum-free culture medium and incubated for 15 min at RT. Transfection was performed by dropwise addition of the PEI/DNA mixture to the cells. Transfection with the empty pcDNA3.1 vector was used to generate control samples. After 24 h, medium was refreshed. Medium was aspirated 48 or 72 h post-transfection and cells were harvested by resuspension in PBS. Cells were pelleted by centrifugation (5 min, 1,000 *g*) and the pellet was washed with PBS. Supernatant was discarded and cell pellets were frozen in liquid nitrogen and stored at -80 °C until sample preparation.

In situ treatment of Neuro-2a cells

Cells were seeded in 6-well plates. *In situ* treatment was initiated 24 h later. Medium was aspirated and serum-free medium containing inhibitor or DMSO as vehicle was added (1.0 % v/v DMSO). After 1 h exposure to treatment medium, the medium was aspirated and cells were harvested and stored as described above until sample preparation.

Whole cell lysate

Cell pellets were thawed on ice, resuspended in cold lysis buffer (20 mM HEPES pH 7.2, 2 mM DTT, 250 mM sucrose, 1 mM $MgCl_2$, 2.5 U/mL benzonase) and incubated on ice (15-30 min). The cell lysate was used for membrane preparation (below) or was diluted to 2.0 mg/mL concentration in cold storage buffer (20 mM Hepes, pH 7.2, 2 mM DTT) for use as whole lysate. Protein concentrations were determined by a Quick Start™ Bradford Protein Assay and diluted samples were flash frozen in liquid nitrogen and stored at -80 °C until further use.

Membrane preparation from overexpression lysate

The membrane and cytosolic fractions of cell or tissue lysates were separated by ultracentrifugation (93,000 *g*, 45 min, 4 °C). The supernatant was collected (cytosolic fraction) and the membrane pellet was resuspended in cold storage buffer by thorough pipetting and passage through an insulin needle. Protein concentrations were determined by a Quick Start™ Bradford Protein Assay and samples were diluted to 2.0 mg/mL with cold storage buffer, flash frozen in liquid nitrogen and stored at -80 °C until further use.

Tissue preparation

Organs were isolated from C57BL/6 mice following standard guidelines as approved by the ethical committee of Leiden University (DEC#13191). Isolated organs were frozen in liquid nitrogen and stored at -80 °C. Organs were thawed on ice and homogenized by a glass stick douncing homogenizer in cold lysis buffer (20 mM HEPES, pH 7.2, 2 mM DTT, 1 mM $MgCl_2$, 2.5 U/mL benzonase). The resulting suspension was centrifuged at 1000 *g* for 5 minutes at 4 °C to get rid of residual solid tissue. The supernatant was centrifuged 45 minutes at 93,000 *g* at 4 °C to separate soluble (cytosol) and insoluble (membrane) fractions. The pellet (membrane) was resuspended in storage buffer (20 mM HEPES, pH 7.2, 2 mM DTT) using an insulin syringe. The protein concentration was measured using a Qubit™ protein assay and was adjusted to 2 mg/mL using storage buffer. The resulting lysates were frozen in liquid nitrogen and stored at -80 °C for later use.

Natural substrate-based fluorescence assay DAGL-α

The diacylglycerol substrate assay was performed as reported previously.[12] Standard assay conditions: 0.2 U/mL glycerol kinase (GK), glycerol-3-phosphate oxidase (GPO) and horseradish peroxidase (HRP), 0.125 mM ATP, 10 µM Amplifu™Red, 5% DMSO in a total volume of 200 µL. The assay additionally contained 5 µg/mL MAGL-overexpressing membranes, 100 µM SAG and 0.0075% (w/v) Triton X-100, with a final protein concentration of 50 µg/mL.

Surrogate substrate assay

The biochemical DAGL-α activity assay is based on the method previously described.[3] 200 µL reactions were performed in flat bottom Greiner 96-wells plates in a 50 mM pH 7.2 Hepes buffer. Membrane protein fractions from HEK293T cells transiently transfected with hDAGL-α (0.05 µg/µL final concentration) were used as hDAGL-α source. Inhibitors were introduced in 5.0 µL DMSO. The mixtures were incubated for 20 minutes before 10.0 µL 6 mM PNP-butyrate (final concentration 0.3 mM) in 50% DMSO was added (final DMSO concentration 5.0%). Reactions were allowed to progress for 30 minutes at 20 °C before OD (420 nm) was measured using a TECAN GENios plate reader. All experiments were performed at N=2, n=2 for experimental measurements and N=2, n=4 for controls.
Z'-factor of each plate was determined for the validation of each experiment, using the following formula: $Z' = 1-3(\sigma_{pc}+ \sigma_{nc})/(\mu_{pc} - \mu_{nc})$. The OD from the positive control (pc: DAGL DMSO), and the negative control (nc: 10 µM THL) was used. Plates were accepted for further analysis when Z' > 0.6. Measurements were corrected for the average absorption of the negative control. The average, standard deviation (SD) and standard error of mean (SEM) were calculated and normalized to the corrected positive control. Data was exported to Graphpad Prism 7.0 for the calculation of the pIC_{50} using a non-linear dose-response analysis with variable slope.

Activity-based protein profiling

For *in vitro* inhibition, lysates (19 µL per sample, 2 µg/µL) were thawed on ice. 0.5 µL of the inhibitor (40x stock in DMSO) or pure DMSO (as vehicle) was added to the sample, vortexed briefly and incubated for 20 minutes at RT. Subsequently, 0.5 µL probe (40x stock in DMSO, final concentration 250 nM for MB064, 500 nM for FP-TAMRA) was added to the proteome sample, vortexed briefly and incubated for 15 minutes at RT. For *in situ* inhibition, the *in situ*-treated cells (19.5 µL whole lysate) were directly incubated with the activity-based probe (40x stock in DMSO, final concentration 2 µM for MB064, 500 nM for FP-TAMRA, 20 min, RT). For *in vivo* inhibition the procedure is identical to *in vitro* inhibition, but the inhibitor incubation is skipped. Final volume in all cases was 20 µL (max. 5% DMSO). The reaction was quenched by the addition of 7.5 µL of 4*Laemmli-buffer (final concentrations: 60 mM Tris (pH 6.8), 2% (w/v) SDS, 10% (v/v) glycerol, 1.25% (v/v) β-mercaptoethanol, 0.01% (v/v) bromophenol blue). 10 µL (14 µg protein) of quenched reaction mixture was resolved on 10% acrylamide SDS-PAGE gels (180 V, 75 min). Fluorescence was measured using a Biorad ChemiDoc MP system (fluorescence channels Cy2 (460-490 nm), Cy3 (520-545 nm), Cy5 (625-650 nm) filters). Gels were then stained using coomassie staining and imaged for protein loading control.

Labeling quantification

Fluorescence quantification was performed using Imagelab 6.0 (Biorad). Intensities were normalized to the DMSO control and corrected for protein loading by coomassie staining. pIC_{50} values were calculated using GraphPad Prism 7.0. For all gel-based pIC_{50} determinations three replicates of each condition were used.

In vivo treatment

The animal experiments were conducted in accordance with the guidelines of the ethical committee of Leiden University (DEC#14137). *In vivo* studies were conducted in C57BL/6 mice. Mice were injected i.p. with the inhibitor dissolved in 18:1:1 (v/v/v) mixture of saline/ethanol/PEG-40 (ethoxylated castor oil, 100 µL injections). For the target engagement study, mice were treated with the compounds for 2 h and euthanized by cervical dislocation. Organs were harvested, flash frozen in liquid nitrogen and stored at -80 °C until sample preparation.

Triazole urea library

The triazole urea library was synthesized and characterized by the European Screening Centre in Dundee, Schotland. The general synthetic procedure is identical to that described for **21** (*vide infra*). Compounds were

purified by preparative HPLC/MS and analysed by H-NMR and LC/MS and only submitted to the library if the purity was > 90%.

Synthetic Methods

General remarks

All reactions were performed using oven- or flame-dried glassware and dry (molecular sieves) solvents. Reagents were purchased from Alfa Aesar, Sigma-Aldrich, Acros, and Merck and used without further purification unless noted otherwise. All moisture sensitive reactions were performed under an argon or nitrogen atmosphere.
^{1}H and ^{13}C NMR spectra were recorded on a Bruker DPX-300 (300 MHz), AV-400 (400 MHz) or DRX-500 (500 MHz). Used software for interpretation of NMR-data was Bruker TopSpin 1.3 and MestreNova 11.0. Chemical shift values are reported in ppm with tetramethylsilane or solvent resonance as the internal standard ($CDCl_3$: δ 7.26 for ^{1}H, δ 77.16 for ^{13}C; ACN-*d*3: δ 1.94 for ^{1}H, δ 1.32 for ^{13}C; MeOD: δ 3.31 for ^{1}H, δ 49.00 for ^{13}C).[14] Data are reported as follows: chemical shifts (δ), multiplicity (s = singlet, d = doublet, dd = double doublet, td = triple doublet, t = triplet, bs = broad singlet, m = multiplet), coupling constants *J* (Hz), and integration.
Liquid chromatography analysis was performed on a Finnigan Surveyor LC/MS system, equipped with a C18 column. Flash chromatography was performed using SiliCycle silica gel type SiliaFlash P60 (230−400 mesh). TLC analysis was performed on Merck silica gel 60/Kieselguhr F254, 0.25 mm. Compounds were visualized using $KMnO_4$ stain (K_2CO_3 (40 g), $KMnO_4$ (6 g), and water (600 mL)) or CAM stain ($Ce(NH_4)_4(SO_4)_4{\cdot}2H_2O$ (ceric ammonium sulfate: 10.0 g); ammonium molybdate (25 g); conc. H_2SO_4 (100 mL); H_2O (900 mL)). Preparative HPLC (Waters, 515 HPLC pump M; Waters, 515 HPLC pump L; Waters, 2767 sample manager; Waters SFO System Fluidics Organizer; Waters Acquity Ultra Performance LC, SQ Detector; Waters Binary Gradient Module) was performed on a Waters XBridgeTM column (5 µM C18, 150 x 19 mm). Diode detection was done between 210 and 600 nm. Gradient: ACN in (H_2O + 0.2% TFA). High resolution mass spectra (HRMS) were recorded by direct injection on a q-TOF mass spectrometer (Synapt G2-Si) equipped with an electrospray ion source in positive mode with Leu-enkephalin (*m/z* = 556.2771) as an internal lock mass. The instrument was calibrated prior to measurement using the MS/MS spectrum of Glu-1-fibrinopeptide B.

(*R,S*)-2-Benzylpiperidine (**67**)

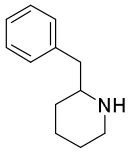

2-Benzylpyridine (5 mL, 31.1 mmol) was dissolved in absolute ethanol (100 mL) and concentrated HCl (10 mL) was added. Then PtO_2 (112 mg, 0.49 mmol) was added and the mixture was shaken under a hydrogen atmosphere of 2 bar at RT. After overnight shaking, solids were filtered off over celite. The solvent was removed under reduced pressure and the residue was purified using silica gel chromatography (10% methanol in DCM) to yield the title compound (4.2 g, 20 mmol, 64%). ^{1}H NMR (300 MHz, $CDCl_3$) δ 8.41 (s, 1H), 7.42 – 7.13 (m, 5H), 3.58 – 3.38 (m, 2H), 3.25 – 3.02 (m, 1H), 3.02 – 2.73 (m, 2H), 2.14 – 1.47 (m, 5H), 1.47 – 1.10 (m, 1H). ^{13}C NMR (75 MHz, $CDCl_3$) δ 136.16, 129.51, 128.76, 127.04, 58.59, 45.11, 40.07, 27.97, 22.61.

3-(Benzylthio)-1*H*-1,2,4-triazole (**69**)

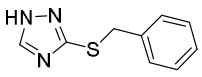

1*H*-1,2,4-Triazole-3-thiol (1.01 g, 10.0 mmol) and benzylbromide (1.09 mL, 10.0 mmol) were dissolved in DMF (10 mL) and stirred for 18 h. The reaction mixture was then diluted with EtOAc (50 mL) and washed with saturated aqueous $NaHCO_3$ (50 mL). The organic phase was separated and the aqueous phase was extracted with EtOAc (50 mL). The combined organic phases were washed with water (50 mL) and brine (50 mL). The volatiles were removed *in vacuo* and the product was obtained as white solid (1.86 g, 9.75 mmol, 98%). ^{1}H NMR (400 MHz, MeOD) δ 8.30 (s, 1H), 7.35 – 7.14 (m, 5H), 4.33 (s, 2H). ^{13}C NMR (101 MHz, MeOD) δ 147.99, 138.64, 129.91, 129.52, 128.48, 37.80.

(2-Benzylpiperidin-1-yl)(3-(benzylthio)-1*H*-1,2,4-triazol-1-yl)methanone (**70**)

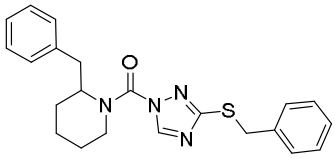

A solution of triphosgene (229 mg, 0.77 mmol) in DCM (5 mL) was cooled to -5 °C, and a solution of **67** (90 mg, 0.51 mmol) in DCM (3 mL) was added dropwise over a period of 5 minutes. To this mixture was added dropwise over a period of 15-30 minutes a solution of TEA (0.21 mL, 1.54 mmol) in DCM (3 mL). The cold bath was removed and stirring at RT was continued for 2 h. The mixture was diluted with DCM (10 mL) and washed with aqueous 1 M HCl (10 mL). The organic phase was separated, dried ($MgSO_4$), filtered and evaporated to dryness. The residue was taken up in DMF (2 mL) to which **69** (32 mg, 0.17 mmol) and K_2CO_3 (116 mg, 0.84 mmol) were added while stirring at RT. After stirring

overnight, the reaction was quenched with water and the product was extracted into EtOAc. The organic phase was evaporated to dryness and the residual material was purified on preparative HPLC to yield the title compound as a yellow gum (22 mg, 54 µmol, 32%). ^{1}H NMR (400 MHz, $CDCl_3$) δ 8.31 (bs, 1H), 7.71 – 6.37 (m, 10H), 4.63 (bs, 1H), 4.38 (d, *J* = 2.5 Hz, 2H), 3.98 (d, *J* = 13.1 Hz, 1H), 3.62 – 3.20 (m, 2H), 3.09 (d, *J* = 3.5 Hz, 1H), 2.95 – 2.38 (m, 2H), 2.02 – 1.33 (m, 4H).

1-(2-Benzylpiperidine-1-carbonyl)-*N*-methyl-*N*-phenyl-1*H*-1,2,4-triazole-3-sulfonamide (**21**)

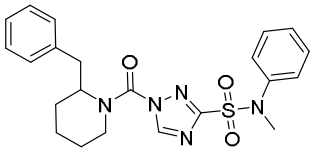

4 M HCl in dioxane (2 mL) was added to DCM (10 mL) and cooled to -10 °C. 15%$_{wt}$ NaOCl solution (aq., 2 mL) was slowly added, a yellow-green colour was observed. After 30 minutes of stirring, **70** (100 mg, 0.255 mmol) in DCM (1 mL) was added slowly. After 30 minutes *N*-methylaniline (2.0 mL, 18 mmol) was added in one batch and stirring was continued for 1 h on ice and 1 h at RT. The DCM was evaporated under reduced pressure and residual solvent was diluted with EtOAc (25 mL) and washed with 0.1 M aqueous HCl (25 mL). The aqueous layer was extracted with EtOAc (2x 25 mL). The combined organic layers were dried ($MgSO_4$), filtered and concentrated. The residue was purified by preparative HPLC to yield the title compound as a green gum (58 mg, 0.13 mmol, 52%). ^{1}H NMR (400 MHz, $CDCl_3$) δ 7.91 (d, *J* = 18.9 Hz, 1H), 7.40 – 6.78 (m, 10H), 4.70 (s, 1H), 4.29 – 4.13 (m, 1H), 3.48 (s, 3H), 3.32 – 3.20 (m, 1H), 3.13 (s, 1H), 2.61 (d, *J* = 18.2 Hz, 1H), 1.74 (m, 6H). HRMS: Calculated for $[C_{22}H_{25}N_5O_3S + Na]^+$ = 462.1570, found = 462.1573.

3-(Benzylthio)-*N,N*-diphenyl-1*H*-1,2,4-triazole-1-carboxamide (**72**)

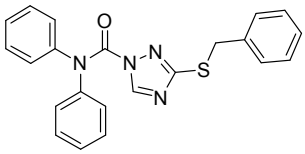

69 (2.137 g, 11.17 mmol) was dissolved in dry THF (40 mL) and diphenylcarbamic chloride (2.85 g, 12.3 mmol), DIPEA (2.34 mL, 13.4 mmol) and a catalytic amount of DMAP were added. The mixture was refluxed for 5 h and stirred for 18 h at RT. The reaction was quenched by the addition of sat. aq. Na_2CO_3 (40 mL). The organic layer was separated and the aqueous phase extracted with EtOAc (2x 40 mL). The combined organic layers were washed with brine (40 mL), dried ($MgSO_4$), filtered and concentrated. Column chromatography afforded the title compound as a white solid (3.81 g, 9.86 mmol, 88%). ^{1}H NMR (400 MHz, $CDCl_3$) δ 8.70 (s, 1H), 7.46 – 7.10 (m, 15H), 3.86 (s, 2H). ^{13}C NMR (101 MHz, $CDCl_3$) δ 162.81, 148.53, 147.18, 142.64, 136.61, 129.58, 129.04, 128.65, 127.60, 127.42, 126.80, 35.89.

3-(*N*-Methyl-*N*-phenylsulfamoyl)-*N,N*-diphenyl-1*H*-1,2,4-triazole-1-carboxamide (**73**)

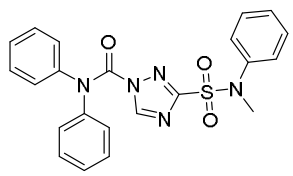

4 N HCl in dioxane (2 mL) was added to DCM (5 mL) and cooled to -10 °C. 15%$_{wt}$ NaOCl (aq., 2 mL) was added slowly, forming a yellow-green Cl_2 solution. After 30 min **72** (100 mg, 0.259 mmol) was added dropwise as a solution in DCM (1 mL). After 20 min *N*-methylaniline (1 mL, 9 mmol) was added. The mixture was stirred for 2 h at RT. The reaction was quenched by the addition of 0.1 M HCl (10 mL). The organic layer was separated and the water layer was extracted with EtOAc (2x, 10 mL). The combined organic layers were dried ($MgSO_4$), filtered and concentrated. The residue was purified by column chromatography to yield the title compound as a brown solid (78 mg, 0.18 mmol, 69%). ^{1}H NMR (400 MHz, $CDCl_3$) δ 8.80 (s, 1H), 7.47 – 6.99 (m, 15H), 3.07 (s, 3H). ^{13}C NMR (101 MHz, $CDCl_3$) δ 160.95, 147.73, 147.28, 141.75, 140.35, 129.45, 128.87, 127.58, 127.47, 126.76, 126.40, 39.02.

N-Methyl-*N*-phenyl-1*H*-1,2,4-triazole-3-sulfonamide (**74**)

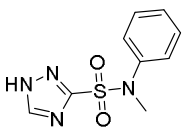

73 (1.05 g, 2.42 mmol) was dissolved in 2 N KOH in a 1:1 (v/v) H_2O/THF mixture (50 mL). The mixture was stirred for 18 h at RT. The mixture was concentrated and the residue was purified by column chromatography to yield the title compound (308 mg, 1.29 mmol, 53%). ^{1}H NMR (400 MHz, MeOD) δ 8.63 (s, 1H), 7.46 – 7.09 (m, 5H), 3.42 (s, 3H).

(2*R*,5*R*)-2-Benzyl-5-(prop-2-yn-1-yloxy)piperidine 2,2,2-trifluoroacetate (**76**)

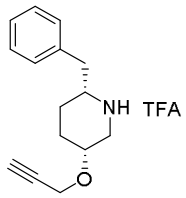

Previously prepared *tert*-butyl (2*R*,5*R*)-2-benzyl-5-(prop-2-yn-1-yloxy)piperidine-1-carboxylate (30 mg, 91 µmol) was dissolved in DCM (6 mL) to which trifluoroacetic acid (2 mL, 26 mmol) was added. The mixture was stirred for 5 h at RT. The volatiles were evaporated and the crude residue was coevaporated with toluene (3x 5 mL) and used without further purification for the next reaction.

1-((2*R*,5*R*)-2-Benzyl-5-(prop-2-yn-1-yloxy)piperidine-1-carbonyl)-*N*-methyl-*N*-phenyl-1*H*-1,2,4-triazole-3-sulfonamide (**77**)

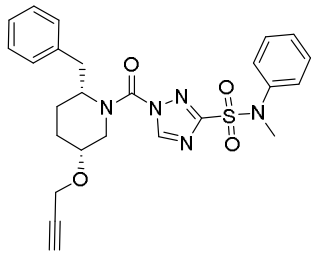

76 (31.3 mg, 0.091 mmol) was dissolved in DCM (5 mL) and cooled to 0 °C. Triphosgene (13.5 mg, 0.046 mmol) and DIPEA (40 µL, 0.30 mmol) were added and the mixture was stirred for 1 h warming to RT. The reaction was quenched with ice water (5 mL) and the organic layer was separated. The aqueous layer was extracted with EtOAc (2x 5 mL). The combined organic layers were dried ($MgSO_4$), filtered and concentrated under reduced pressure. The crude was taken up in dry THF (5 mL) and **74** (24 mg, 0.10 mmol), DMAP (11 mg, 0.091 mmol) and DIPEA (40 µL, 0.30 mmol) were added. The mixture was refluxed for 5 h. The reaction was quenched with saturated aqueous NH_4Cl (5 mL). The organic layer was diluted with EtOAc (5 mL) and separated. The aqueous layer was extracted with EtOAc (2x 10 mL). The combined organic layers were washed with brine, dried ($MgSO_4$), filtered and concentrated *in vacuo*. The residue was purified by flash column chromatography to yield the title compound as a white solid (30.2 mg, 61 µmol, 67%). ^{1}H NMR (400 MHz, $CDCl_3$) δ 7.99 (s, 1H), 7.42 – 6.78 (m, 10H), 4.71 (s, 1H), 4.48 (s, 1H), 4.30 (s, 2H), 3.79 – 3.62 (m, 1H), 3.52 (s, 3H), 3.21 – 2.99 (m, 2H), 2.67 (s, 1H), 2.49 (s, 1H), 2.10 (d, *J* = 19.3 Hz, 1H), 1.80 (d, *J* = 11.8 Hz, 3H). HRMS: Calculated for $[C_{25}H_{27}N_5O_4S + Na]^+$ = 516.1676, found = 516.1680.

Supplementary Figures

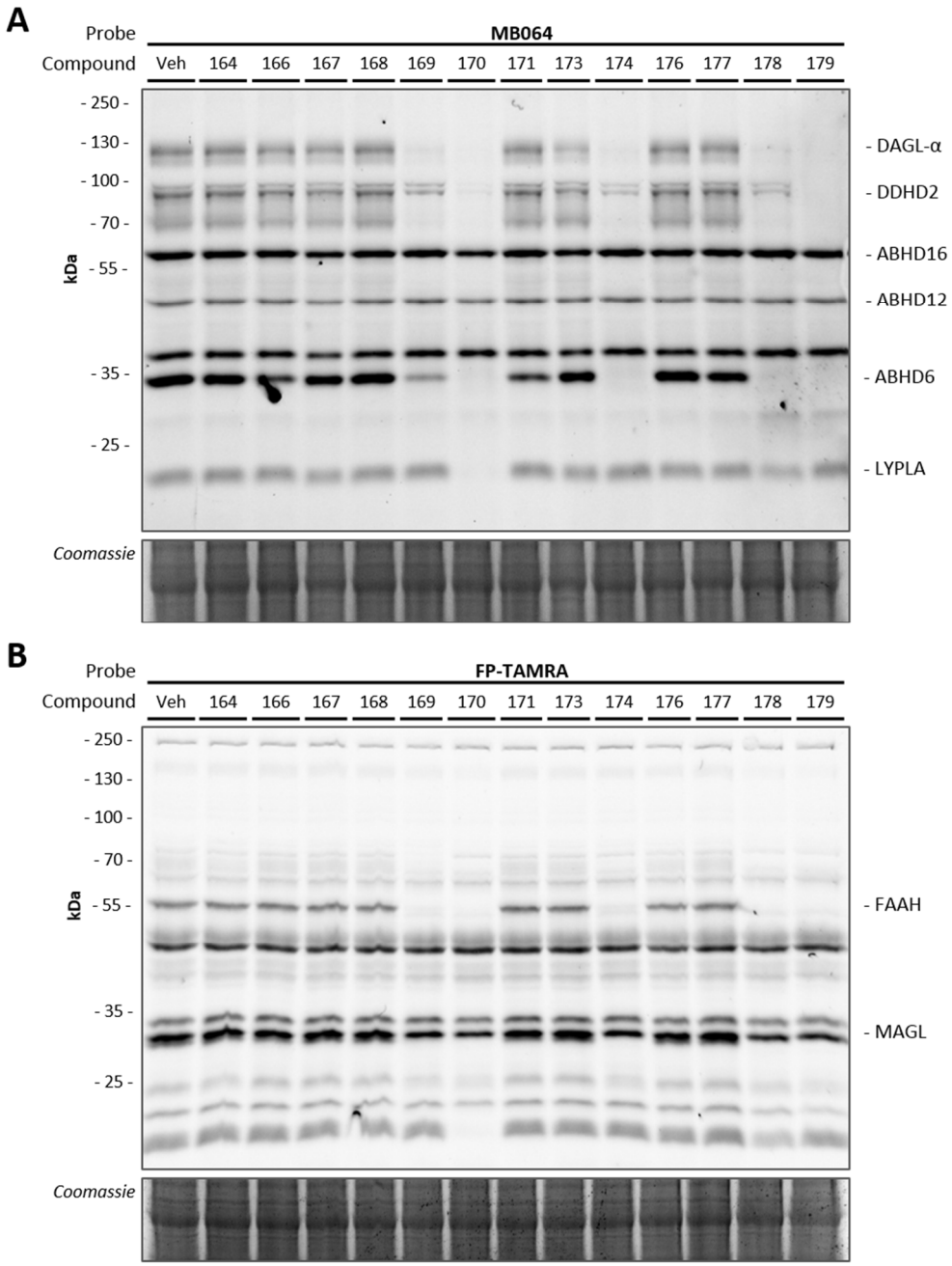

Figure S2.1 | Typical off-target profiling screen using MB064 (A) and FP-TAMRA (B). Compound numbers correspond to compound ESC-library codes. Compounds were screened at a concentration of 10 μM.

References

1. Hsu, K. *et al.* DAGLβ inhibition perturbs a lipid network involved in macrophage inflammatory responses. *Nat. Chem. Biol.* **8**, 999–1007 (2012).
2. Janssen, F. J. & van der Stelt, M. Inhibitors of diacylglycerol lipases in neurodegenerative and metabolic disorders. *Bioorg. Med. Chem. Lett.* **26**, 3831–3837 (2016).
3. Baggelaar, M. P. *et al.* Development of an Activity-Based Probe and In Silico Design Reveal Highly Selective Inhibitors for Diacylglycerol Lipase-α in Brain. *Angew. Chemie Int. Ed.* **52**, 12081–12085 (2013).
4. Baggelaar, M. P. *et al.* Highly Selective, Reversible Inhibitor Identified by Comparative Chemoproteomics Modulates Diacylglycerol Lipase Activity in Neurons. *J. Am. Chem. Soc.* **137**, 8851–8857 (2015).
5. Janssen, F. J. *et al.* Discovery of Glycine Sulfonamides as Dual Inhibitors of sn -1-Diacylglycerol Lipase α and α/β-Hydrolase Domain 6. *J. Med. Chem.* **57**, 6610–6622 (2014).
6. Hu, S. *et al.* Glycine chroman-6-sulfonamides for use as inhibitors of diacylglycerol lipase. US-patent US 8354548 B2. (2011).
7. Ogasawara, D. *et al.* Rapid and profound rewiring of brain lipid signaling networks by acute diacylglycerol lipase inhibition. *Proc. Natl. Acad. Sci.* **113**, 26–33 (2016).
8. Deng, H. *et al.* Triazole Ureas Act as Diacylglycerol Lipase Inhibitors and Prevent Fasting-Induced Refeeding. *J. Med. Chem.* **60**, 428–440 (2017).
9. Chupak, L. S. *et al.* Structure activity relationship studies on chemically non-reactive glycine sulfonamide inhibitors of diacylglycerol lipase. *Bioorg. Med. Chem.* **24**, 1455–1468 (2016).
10. Janssen, F. J., Discovery of sulfonyl-1,2,4-triazole ureas as DAGLα inhibitors by HTS-ABPP. in *Discovery of novel inhibitors to investigate diacylglycerol lipases and α/β-hydrolase domain 16A* 109–139 (2016).
11. Hsu, K.-L. *et al.* Development and Optimization of Piperidyl-1,2,3-Triazole Ureas as Selective Chemical Probes of Endocannabinoid Biosynthesis. *J. Med. Chem.* **56**, 8257–8269 (2013).
12. van der Wel, T. *et al.* A natural substrate-based fluorescence assay for inhibitor screening on diacylglycerol lipase α. *J. Lipid Res.* **56**, 927–935 (2015).
13. van Esbroeck, A. C. M. *et al.* Activity-based protein profiling reveals off-target proteins of the FAAH inhibitor BIA 10-2474. *Science* **356**, 1084–1087 (2017).
14. Gottlieb, H. E., Kotlyar, V. & Nudelman, A. NMR Chemical Shifts of Common Laboratory Solvents as Trace Impurities. *J. Org. Chem.* **62**, 7512–7515 (1997).